

# THERMAL MAPPING OF SRF CAVITIES BY SECOND SOUND DETECTION WITH TRANSITION EDGE SENSORS AND OSCILLATING SUPERLEAK TRANSDUCERS

G. Vandoni, T. Koettig, A. Macpherson, K. M. Turaj, L. Vega Cid, CERN, Geneva, Switzerland  
H. Furci, EPFL, Lausanne, Switzerland

## Abstract

The Superconducting Radio Frequency (SRF) cavity testing facilities at CERN include four vertical cryostat stations in SM18 and a cryostat for small cavities in the Cryolab. A large range of structures are tested, from Nb thin film cavities for HIE-Isolde and LHC, to bulk Nb crab cavities for HiLumi or 704 MHz 5-cell high-gradient cavities. To cope with different shapes and small series tests, thermal mapping diagnostics is deployed by sensing second sound in superfluid helium. A new type of Transition Edge Sensors (TES) has been developed in the last 2 years. These are miniature resistors of thin-film superconducting alloys, micro-produced on insulating wafers. An extensive campaign of optimization of design, fabrication process and composition was accompanied by qualification in a calibration cryostat. Reproducibility, stability, then intensity, distance and angular dependence of the response were assessed and compared to Oscillating Superleak Transducers (OST). The TES were then installed in a vertical cryostat for tests of a prototype crab cavity for HiLumi. TES are now applied to quench localization on high gradient cavities, for which the most recent results will be presented, together with the OST results.

## INTRODUCTION

Superconducting RF single cavity testing is a key activity in the development and production of SRF cavities at CERN. A wide variety of cavities have been tested at 4 K and 2 K in the last years in the 4 vertical cryostats of the SM18 facility, from 1.3 GHz elliptical cavities, to quarter-wave resonators in Nb thin film on copper for HIE-Isolde and bulk niobium crab-cavities for the High Luminosity LHC project. A widespread diagnostics method amongst SRF laboratories, thermal mapping is used in cavity testing facilities to localize defects acting as quench departure spots. For defect localization on LEP cavities, the thermal mapping system consisted in a set of carbon resistor thermometers, mounted on a rotating frame and kept touching the cavity wall by springs [1]. Large arrays of thermometers mounted on PCB boards matching the form of the cavity are used in several laboratories for monitoring series production of elliptical cavities [2]. Actually, contact thermometry is adequate for thermal mapping of large series of identical, convex, rotational symmetry cavities. However, for a small number and large variety of cavities with locally concave surface, it is better to resort to contactless thermal mapping, based on transmission of the local heat pulse via the helium bath. For cavities operated and tested in superfluid helium, the detection of second sound has thus proven to be a suitable tool for localization of hot

spots, once the signal on different second sound sensors has been deconvoluted by trilateration algorithms.

In the two-fluid description of a superfluid, second sound is the oscillation of the normal and superfluid components in counterflow, without density change: a thermal excitation, or entropy wave, driven by temperature difference. This powerful mechanism of heat transfer has a characteristic propagation velocity of 20 m/s at 1.8 K, with velocity quickly dropping from 1.9 K to 2.18 K, but remaining constant between 1.9 K and 1 K, before rising exponentially at lower temperature. Second sound propagation is commonly used in hydrodynamic experimental studies on superfluid helium, either as travelling or as standing wave. Second sound attenuates as a function of the interaction forces between the two-fluid components, allowing the study of vortex formation, laminar-to-turbulent flow onset, etc.

Typically, second sound is detected by either very sensitive thermometry, or by filtering the superfluid component in a semi-porous oscillating membrane in a capacitive sensor. The latter effect is used in oscillating superleak transducers, (OST) [3], commonly applied in SRF localization of quenches [4], where the localization of the quench relies on the measurement of the travelling time between the heat source and each sensor. OSTs are however limited in spatial and time resolution due to their centimetre-scale size. Thermometric detection of second sound has also been applied to quench localization [5] in SRF cavities.

Our work presents the development of new thin-film thermometric probes, tailored to SRF needs. By their reduced dimensions and mass (see Fig. 1), these sensors, based on thin-film superconducting alloys, are able to detect temperature variations of  $< 1\text{mK}$  with rise time  $< 1\ \mu\text{s}$ .

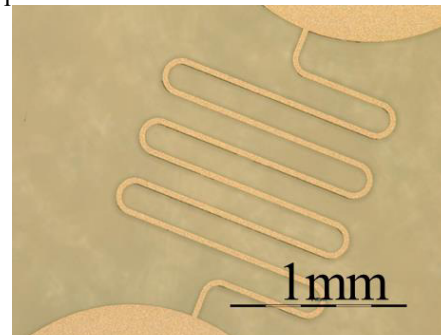


Figure 1: Micro photography of a thin film Transition Edge Sensor with 225 nm Sn on 20 nm Au.

Alloying transforms the sharp superconducting to normal conducting transition curve by lowering the resistance versus temperature slope at the transition. The sensors can be current-biased, thus lowering the

superconducting transition edge to match the superfluid bath temperature. The miniature thin-film sensors can then be used as bolometers, sensing entropy waves in the superfluid helium bath.

In the next sections, we present the development of Transition Edge Sensors (TES) at CERN. We then report on how they have been successfully applied for quench localization on a double-quarter wave crab cavity.

## THIN-FILM AU-SN TRANSITION EDGE SENSORS

Superconducting alloy thin films have been studied as second-sound sensors for photon detection since the '70ies [6], where fabrication by photolithography was developed and the combination of gold and tin identified as featuring the best sensitivity, stability and reproducibility. Probe design and composition optimization were further developed in [7]. Several laboratories now prepare their own TES in house, with design adapted to the phenomenon under scrutiny.

We developed a fabrication process based on state-of-the-art photolithography techniques, to obtain sensors with an active area of the order of  $<1 \text{ mm}^2$ . Several sensors can be produced on a wafer (Fig. 2) or as single sensors, which are then installed in a holder (Fig. 3). The sensors were then characterized in a 2 K cryostat, using point heaters as second sound sources.

### Production Procedure

The thin films are deposited on a borosilicate glass flat wafer. The wafer is first coated with a double layer of lift-off resin and photoresist. The design of the  $1 \mu\text{m}$  precise pattern of TES sensors with connection pads is drawn in negative on the photoresist by a UV laser. Then, the pattern is developed using a solvent, resulting in a structured polymer layer with voids corresponding to the expected final pattern of the thin film.



Figure 2: TES wafer used for cavity diagnostics.

The thin film is obtained by evaporating gold, then tin, in a vacuum oven, at a rate of  $0.3 \text{ nm/s}$ , until the required thickness is obtained. Thickness is monitored by a calibrated quartz oscillator. Lift-off of the resin is then performed in a remover solvent bath.

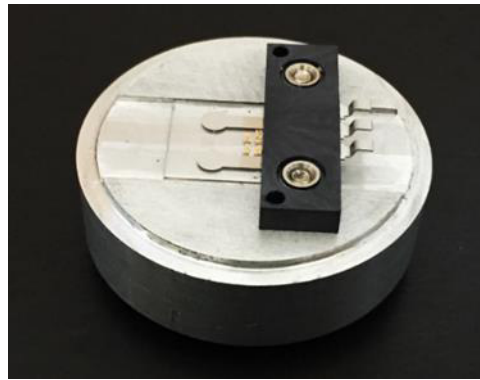


Figure 3: Single TES on disk support and cable pad.

The above procedure results in several sensors on a single wafer, which may then be used as an extended surface “camera”. To have single sensors, the wafer is pre-diced before starting the process; once the process completed, it is easy to cut the wafer into single-sensor portions. A microscopy image of a single sensor is shown on Fig. 1, while a wafer with 30 sensors is shown on Fig. 2 and a single sensor assembled in a circular support is shown on Fig. 3.

### Experimental Characterization

Validation and characterization of the TES is performed in a cryogenic open bath cryostat, operated with saturated superfluid helium. The sensor’s holder is attached to the top-plate of the cryostat, below a set of thermal screens. Pressure is lowered to saturated superfluid conditions by pumping via a regulation valve controlled by a pressure transducer with  $5 \text{ Pa}$  precision. The lowest temperature obtained with this system is  $1.5 \text{ K}$ .

To characterize the TES, on wafers with multiple sensors or as individual sensors, the voltage-to-current characteristics is measured between  $1.6 \text{ K}$  and  $2.0 \text{ K}$ . Temperature is first stabilized at the required value, then current is swept slowly while reading voltage. Next, temperature is incremented, in  $50 \text{ mK}$  steps. Finite differentiation provides the voltage to temperature sensitivity. The operational bias current at each temperature is then chosen as the one corresponding to the sensitivity peak. The best characteristics, with a smooth S-shape and good sensitivity, was obtained with thin film sensors produced by depositing  $20 \text{ nm Au}$ , then  $225 \text{ nm Sn}$ . Fig. 4 displays the characteristics and sensitivity curve of one of these sensors. This composition was finally chosen for the production of a series of TES, both as wafers with 30 sensors and as diced, individual sensors.

Second sound detection was obtained in the same cryostat, by biasing the TES to their optimal current, then generating a heat pulse produced by SMD thick film resistors and sensing the time response of the sensors [8]. Comparative measurement with OST of the response to a heat pulse as a function of orientation angle with respect to the normal vector of an extended flat heater were also performed.

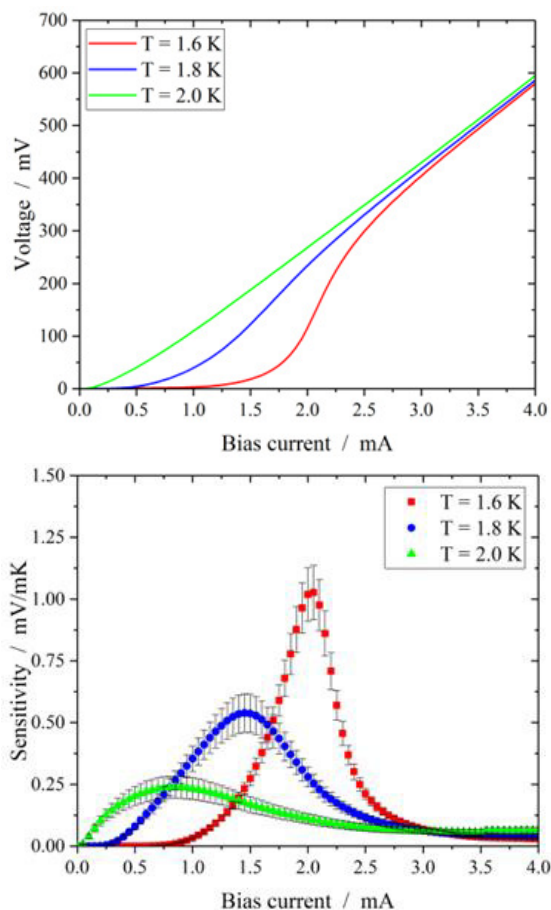


Figure 4: Characteristics (upper) and sensitivity (lower figure) of TES versus bias current, at 3 temperatures.

The TES yielded a lesser angular dependence with respect to OST, proving their superiority for quench localization from the rounded surfaces of SRF cavities (Fig. 5).

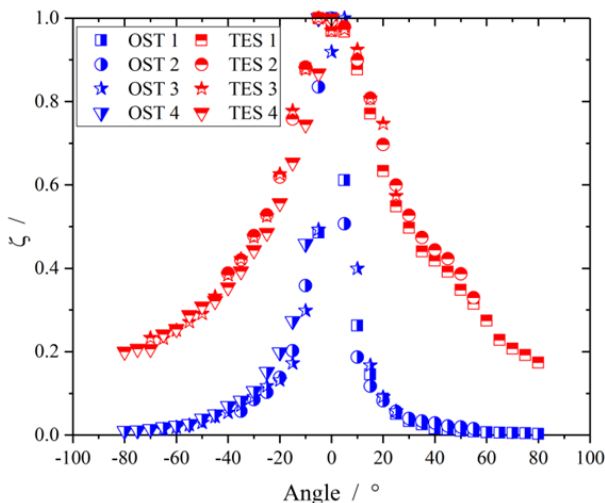


Figure 5: Normalized signal from four OSTs and four TES, plotted as a function of the angle between the normal vectors of sensor and heater surface.

## TES USE IN CAVITY TEST

Two wafers with 30 TES each have been installed on one of the vertical test stands in SM18 and operated during test of a prototype, 400 MHz Double-Quarter Wave (DQW) crab cavity, developed in the framework of the High Luminosity LHC project [9]. The cryostat is a 4-metre deep, open bath helium vessel connected to the helium distribution system of SM18, which supplies liquid helium and provides the pumping to saturated superfluid conditions. Cavities under test are supported from the cryostat insert, itself fixed to the top-plate, outfitted with passively cooled thermal screens and cavity pumping line.

The DQW cavity is mounted in a stiffening frame and tested in horizontal orientation; the two wafers are attached to the insert's assembly disks via composite stand-offs and positioned at the centre of the cavity capacitive plates above and below the cavity. Fig. 6 shows the upper TES wafer facing the cavity. Due to limited feedthrough ports availability, only 4 TES were cabled on each wafer.



Figure 6: Upper wafer in its support, facing the cavity.

### Test Results and Hot-Spot Localization

The cavity was tested at 1.75 K - 1.8 K. In this temperature range, second sound speed is constant at  $20.0 \pm 0.1$  m/s. Reporting the cavity RF performance is beyond the scope of this work, some results are given in [10].

The 8 TES are biased with the current yielding maximum sensitivity for the bath temperature. Voltage is read via a NI9251 acquisition card with sampling rate 50 kHz. As RF power is supplied to the cavity, the transmitted power signal from the pick-up antenna is also recorded with the same DAQ system as the TES, to provide for zero time reference and transmitted power resolved in time. A LabView interface controls acquisition and data storage; data buffering is triggered by any chosen RF power signal, when a change larger than a pre-defined threshold is exceeded.

After conditioning, RF power is ramped up. The cavity quenches at 38 W, with a pulsating quench behaviour. Transmitted power first increases as the cavity loads up, then after  $\sim 1$  s the cavity uploads, while reflected power increases with time constant  $\sim 10$  ms, then slowly decays as the cavity loads up again. This behaviour repeats itself, with a frequency of 0.7 Hz; as the quench occurs, the cavity dissipates and releases its stored energy, allowing the

quench spot to cool and return to the superconductive state, such that the cavity refills with energy, before quenching again.

Any signal recorded at the TES wafer positioned below the cavity during these repeated quenches is too small to rise above noise. Instead, all four TES above the cavity react with good signal-to-noise ratio to the pulsating quench.

Cavity power balance allows to determine dissipated power and to plot its time variation and second time derivative (Fig. 7 above). Dissipated power  $P_c$  is

$$P_c = P_f - P_t - P_r - \kappa \frac{\partial P_t}{\partial t} \quad (1)$$

with  $\kappa P_t$  stored energy in the cavity. The time variation of the second sound perturbation wave,  $q''$ , with  $u_{ss}$  second sound velocity,  $\rho$  helium density and  $C$  heat capacity, is proportional to the time variation of dissipated power:

$$\frac{1}{\rho C u_{ss}} \frac{\partial q''}{\partial t} \propto \frac{dP_c}{dt} \approx -\kappa \frac{d^2 P_t}{dt^2} \quad (2)$$

Rather than a steeply rising second-sound signal, the TES hence feature a response rising with the same time profile (Fig. 7 below). The time-of-flight of the generated entropy wave in the superfluid, from the dissipation spot to each of the TES, is therefore deconvoluted with the time profile of dissipated power having generated second sound.

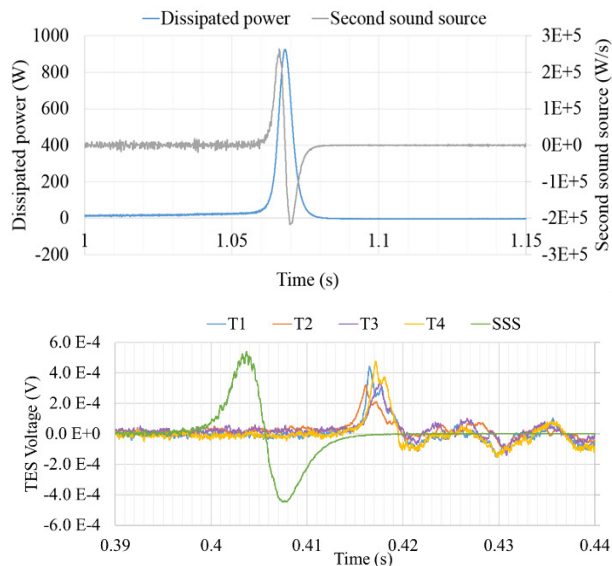


Figure 7: Above: Dissipated power and its time derivative, or second sound source. Below: second sound source signal (green, arb. units) and response of the four TES sensors above the cavity.

Thanks to the repetition of successive quenches, a statistical analysis on the TES data becomes possible. To maximize trilateration precision in spite of the small distance between the sensors, instead of using the time lag between the source signal and each TES, we compute arrival time differences, or lags, between the sensors and

sum each time lag to the average lag between the source and all TES. With four sensors, three sets of trilateration position definitions are possible. The three obtained positions are shown on Fig. 8; they lie within an area of 2 cm diameter, close to the capacitive plate, in a zone of minimal concavity radius. The exact location obtained by trilateration appears as slightly inside the volume of the cavity.

### Discussion

The pulsating quench appears as being initiated in an area of high electric field. This fact suggests that the origin of the local heating is electron bombardment from field-emitted electrons. Locating the origin of this field emission would require electron trajectory simulations, with the hot spot as target position.

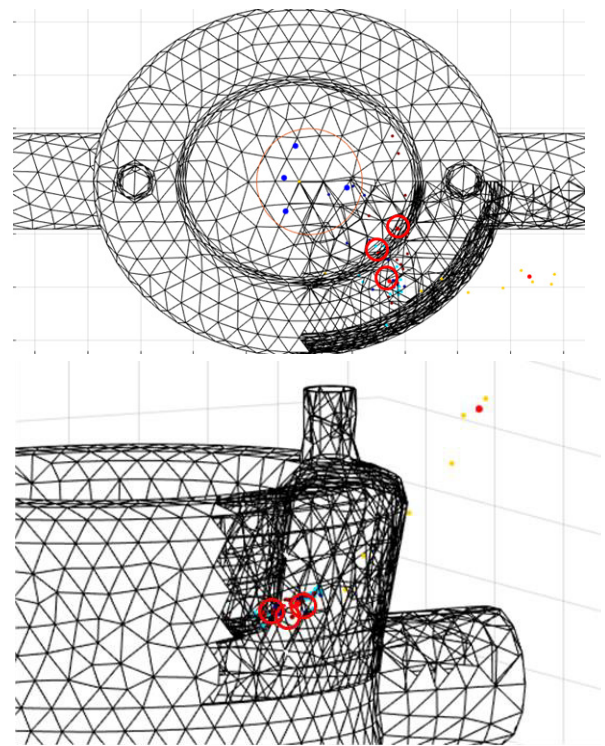


Figure 8: Trilateration algorithm applied to four TES results in identification of 3 candidate sources of second sound. These are in a high electric field zone.

The fact that the second sound source appears as *inside* the cavity is certainly a measurement analysis artefact. Due to the presence of the stiffening frame, second sound waves are deviated from the source to the sensors; trilateration calculates the shortest, non-deflected path, as having its source at a larger distance than the cavity surface. A complete wave-propagation model taking into account the presence of all obstacles would be required to avoid this type of errors.

## CONCLUSIONS AND OUTLOOK

Thin-film Transition Edge Sensors developed at CERN have demonstrated their potential for thermal mapping on

SRF cavities by second sound detection in superfluid helium. These thin-film alloy sensors, biased through the edge of the superconducting to normal transition to match helium bath temperature, are highly sensitive, feature an excellent space and time resolution and are superior to OST in being less sensitive to orientation mismatch. In the form of multiple sensors on a single wafer, they have been successfully applied to the localization of the origin of a pulsating quench in a proof-of-principle DQW crab cavity.

Improving the method by a larger separation between sensors than what is allowed by multiple TES on a single wafer, single TES have subsequently been installed around a high-gradient 5-cell 704 MHz cavity. Measurements on this cavity are imminent. To improve localization of quench spots, some point heaters have been installed on fiducialized positions on the cavity. Prior to each measurement, it becomes therefore possible to localize the TES with respect to the cavity in an inversed trilateration. With the data acquisition software operating, we hope to be soon able to extend the use of TES as a powerful diagnostics tool in SRF cavity testing at 2 K.

## REFERENCES

- [1] Ph. Bernard *et al.*, “Experiments with the CERN Superconducting 500 MHz Cavity”, *Nucl. Instr. Meth.*, vol. 190, pp. 257-282, 1981.
- [2] G. M. Ge and G. H. Hoffstaetter, “A Temperature-Mapping System for Multi-Cell SRF Accelerator Cavities”, in *Proc. North American Particle Accelerator Conf. (NAPAC’13)*, Pasadena, CA, USA, Sep.-Oct. 2013, paper WEPAC09, pp. 805-807 and references therein.
- [3] R.A. Sherlock and D.O. Edwards, “Oscillating Superleak Second Sound Transducers,” *Rev. Sci. Instrum.* 41, p. 1603 (1970).
- [4] Z. A. Conway, D. L. Hartill, H. Padamsee, and E. N. Smith, “Defect Location in Superconducting Cavities Cooled with HE-II Using Oscillating Superleak Transducers”, in *Proc. 14th Int. Conf. RF Superconductivity (SRF’09)*, Berlin, Germany, Sep. 2009, paper TUOAAU05, pp. 113-116.
- [5] M. P. Kelly, M. Kedzie, and Z. C. Liu, “A Simple Second Sound Detection Technique for SRF Cavities”, in *Proc. 14th Int. Conf. RF Superconductivity (SRF’09)*, Berlin, Germany, Sep. 2009, paper TUPPO032, pp. 273-275.
- [6] G. Laguna, “Photolithographic Fabrication of High Frequency Second Sound Detectors”, *Cryogenics*, Volume 16, 1976, 241-243.
- [7] H. Borner, T. Schmeling, D.W. Schmidt, “Experimental Investigations on Fast Gold-Tin Metal Film Second-Sound Detectors and their Application”, *Journal of Low-temperature Physics*, Vol.50, 1983, 405-426.
- [8] H. Furci *et al.*, “Heat Source Localisation by Trilateration of Helium II second sound detected with transition edge sensors thermometry”, in *Proc. ICEC’18, IOP Conf. Ser.: Mater. Sci. Eng.* **502** 012115. doi.org/10.1088/1757-899X/502/1/012115
- [9] G. Apollinari *et al.*, “High-Luminosity Large Hadron Collider (HL-LHC): Technical Design Report v.0.1”, in *CERN Yellow Reports: Monographs*, CERN, Switzerland, 2017.
- [10] R. Apsimon *et al.*, “Prediction of beam losses during crab cavity quenches at the high luminosity LHC”, *Phys. Rev Accelerators and Beams*, vol. 22, 061001, 2019